Article ID: 1000-9116(2008)01-0035-11 doi: 10.1007/s11589-008-0035-5

Synthetic study on SS waveform splitting and complication*

HE Xiao-bo[1),♣] (何小波) ZHOU Hui-lan[1)] (周蕙兰) MA Yan-lu[1)](马延路)
NIU Feng-lin[2)] (钮凤林)

1) *Computational Geodynamic Laboratory*, *Graduate University of Chinese Academy of Sciences*, *Beijing* 100049, *China*
2) *Department of Earth Science*, *Rice University*, *Houston* 77006, *USA*

Abstract

Some influential factors on the complication of SS waveform (with epicentral distance within 40°~180°) are analyzed quantitatively by calculating the full-wave synthetic seismogram using propagation matrix method. Our results show that the transmission-conversion and reflection-conversion phases of S wave at the interface of Moho and free surface beneath bounce points are mainly responsible for the complication of SS waveform, the velocity contrast between the two sides of Moho boundary under SS bounce point also has great effects on the amplitudes of all the conversion and the reverberation phases; the properties of the crust at seismic station also play a role in the complication of SS waveform while the crustal thickness beneath bounce point is thinner relatively. At the same time, two sets of real SS waveform data at the two positions in eastern and western China are analyzed, and the splitting time between SS transverse component and radial component is measured by cross-correlation. Our analysis demonstrates that there is a positive correlation between crustal thickness and the splitting time because of the influences of adjacent conversion and reverberation phases, the splitting time in west with thick crust is obviously greater than that in the east with thin crust. Moreover, It is promising that one new method of measurement of crustal thickness will be developed by using the observed SS splitting time.

Key words: **SS waveform**; **splitting time**; **crustal thickness**; **synthetic seismogram**; **Green's function**
CLC number: P315.3^{+}1 **Document code**: A

Introduction

Generally the interior structures of the Earth are detected by seismic wave, especially S wave with strong energy is very important to the detection of the deep Earth. However, earthquakes and seismic stations are not distributed evenly, it leads to uneven samples for the Earth's interior structures by direct P and S waves, which are generated from the earthquake source and recorded at stations. In order to improve such distributions and increase record samples, lots of other seismic phases have been added, such as PP, SS, PcP, ScS, PKP and so on. Among these waveforms, many researchers choose SS wave because of its strong energy. For example, SS wave is used to do some researches on the anisotropy in the crust and upper-mantle at its bounce point (Yang and Fischer, 1994; Wolfe and Silver, 1998), global and large scale mantle tomography of S wave (Grand, 2002), the *Q* value distribution of S wave in the crust and upper-mantle (Bhattacharyya *et*

* **Received** 2007-05-07; **accepted in revised form** 2007-11-26.
Foundation item: National Natural Science Foundation of China (40574024 and 40374009).
♣ **Author for correspondence**: xbhe@mails.gucas.ac.cn

al, 1996; Reid *et al*, 2001). At the same time, together with the arrival time difference of SdS on '410'and '660' discontinuities of upper-mantle, SS wave has been used to the researches on topography of global upper-mantle discontinuities and distribution for the thickness of transition zone (Lawrence and Shearer, 2006; Schmerr and Garnero, 2006). Because the waveform of transverse component of SS wave is simple, transverse component is usually used during the researches on tomography, Q value distribution and upper-mantle discontinuities topography.

However, when using SS waveform on both of transverse and radial components, it's necessary to have a deep understanding of the complication of radial waveform. Here, so-called SS waveform is the reflection wave series, such as reflection wave after one time reflection, the wave-train on the Moho interface combined with reflection seismic phases, transmission seismic phases, and multi-reflection seismic phases and multi-conversion seismic phases in crust located in hypocenter area, reflection area and station area. All of these waves among the wave-train have a similar arrival time compared with the original SS wave, so what we see on the seismogram is the combination of them. So when we use the SS waveform to do researches about crustal structure in any of the three sections: hypocenter area, reflection area and seismic station area, we have to focus on one of them, but do not neglect to consider the effect of the rest ones. In this paper, our goal is mainly to discuss the contribution of seismic station and bounce point to the complication of SS waveform. In this case, the contributions of earthquake source's multi-ruptures and the triplication of the original SS seismic phase in certain distances to the complication of SS waveform are ignored.

1 Method

The SS wave-train recorded at seismic station can be expressed as follows:

$$U_{SS}(t) = W(t) * G(t) * I(t) \tag{1}$$

Where $U_{SS}(t)$ is the recorded waveform, $W(t)$ is the time function of the earthquake source, $G(t)$ is the response of medium, called Green's function, $I(t)$ is the response of the seismic instrument. So $G(t)$ can be expressed as

$$G(t) = G_1(t) * G_{r1}(t) * G_2(t) * G_{rc}(t) \tag{2}$$

Where $G_1(t)$ is the medium response from hypocenter to bounce point on Moho interface. It includes the response of crust in hypocenter area when hypocenter is in the crust. $G_{rl}(t)$ is the response of crust C_{rl} on the bounce point. $G_2(t)$ is the medium response from Moho interface under bounce point to Moho interface under seismic station. $G_{rc}(t)$ is the response of crust at seismic station C_{rc}.

In order to focus on the influence of C_{r1} and C_{rc} to SS-waveform's complication, simple crustal model with an upper one layer homogeneous crust in half-infinite space can be used for such cases. Firstly, we choose earthquake with focal depth of about 590 km as one example, which simplifies the problem because its SS waveform generated by source at this depth is simple, and effect of crustal structure in the source area can be neglected. Thus, we just need to care the effects of the crustal structure in the other two areas on the complication of SS waveform. Secondly, only SS waveforms with distance larger than 40° are calculated, which avoids the influence of the triplication of original SS seismic phase on the complication of SS waveform. In addition, relative to large distances from 40° to 180°, the thicknesses (H_{r1} and H_{rc}) of C_{r1} and C_{rc} are very small com-

pared with the length of SS ray path. The seismic phase of the original SS, the reflection and transmission transform SS seismic phases on Moho interface in reflection and seismic station areas and the multi-reflection and reflection transformation SS seismic phase in the crust have similar ray parameters, which can be assumed to be equal. It means they have a same incident angle on the Moho interface. As a result, when discussing the effect on SS waveform's complication of C_{r1} and C_{rc} separately, the model with an upper one-layer homogeneous crust in half-infinite space is used for simplification.

In this paper, full-wave synthetic seismogram is used to analyze SS-waveform's complication quantitatively. When considering the effect of C_{r1}, Ma *et al*'s method (2008) is used to calculate the Green's function and theoretical waveform of the simple crustal model in half-infinite space with an upper one-layer homogeneous crust. However, only considering the effect of C_{rc} on original SS wave is meaningless, because we want to understand the general effect of C_{rc} to a set of SS wave complicated by C_{r1} by comparing with the observed SS-waveform. For this reason, here Wang's method (1999) and the software Qseis5.6 have are used to generate SS synthetic seismograms given different crustal thickness at seismic station, then we can have a look into some influential factors.

During analyzing the real data of SS waveform with large crustal thickness of reflection (reflection on the continent), the theoretical waveform's cross-correlation is used to calibrate the splitting time between SS transverse and radial component. Then we discuss the relationship between splitting time and the crustal thickness under bounce point.

2 Crust on bounce point and the complication of SS wave-train

2.1 Green's function of crust on bounce point

When discussing Green's function of crust on bounce point, we use a simple model: Assuming S wave's incidence is from half-infinite space with an upper one-layer homogeneous crust. The thickness of crust (H_{r1}) is 30 km. The P wave velocity v_P, the S wave velocity v_S and the density of the crust are 6.10 km/s, 3.52 km/s and 2.8 g/cm^3 respectively. While under Moho interface, they are 8.04 km/s, 4.60 km/s and 3.32 g/cm^3 respectively. The Green's function, $G_{r1}(t)$, to S incidence in this crustal model at distance 110° is showed in Figures 1a and 1b. According to theoretical arrival time and slowness, the ray path of main seismic phases is showed in Figure 1c. Because seismic phases are shear wave before and after propagation through the crust beneath bounce point, we simply to indicate seismic phases according to the wave mechanics property through inner crust and the number of times of propagation between Earth surface and Moho interface. For example, 2S stands for S wave comes into crust from Moho interface, reflects by Earth surface, becomes S wave, and comes out from Moho interface, which means there are twice S wave propagations in crust. This is that we called the original SS seismic phase. Likewise, 1P1S stands for propagation as P wave and S wave each for once in crust; 2P2S stands for propagation as P wave and S wave each for twice in crust; 4S stands for propagation as S wave for 4 times. This indication method considered the times of propagation as P wave or S wave in crust without considering the propagation sequences. So when there are both P wave and S wave in crust, it represented one set of seismic phases. For example, 1P1S actually includes two seismic phases. One's generation is that S wave transmits to P on Moho interface, reflects by Earth surface, becomes S wave and comes out of Moho interface. Another one's generation is that S wave transmits on Moho interface into crust, reflects by Earth surface, turns to P wave, arrives at Moho interface

and transmits to S wave. The travel times of the two seismic phases are the same but with different energy. The number of seismic phases recorded as 2P2S is larger.

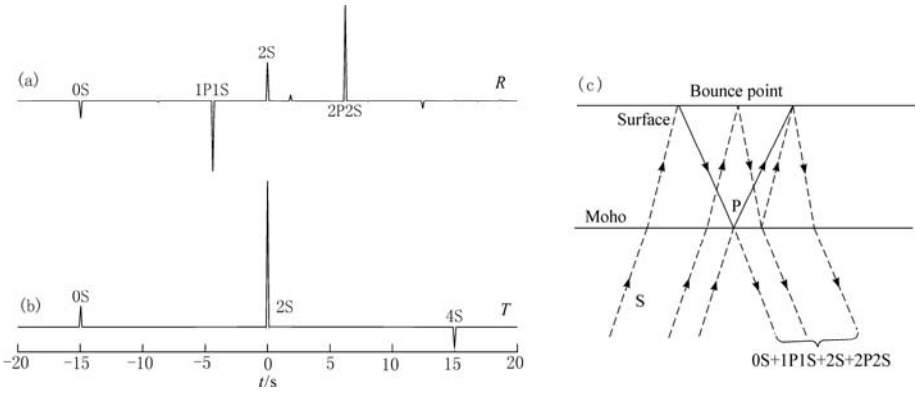

Figure 1 SS Green's function and schematic ray path beneath bounce point
(a) and (b) represent Green's functions of radial and transverse component respectively. Several main seismic phases are marked in the figure; (c) shows SS wave-train's ray path at the bounce point in crust. Dash lines stand for S wave, while solid lines stand for P wave. Crustal thickness H_{r1} is 30 km, distance Δ is 110°

Because there is a transform relationship between SV and P wave, 1P1S and 2P2S just appeared on Green's function for R component (R_{SS}) of SS waveform, and the energy they bring is larger than 2S. 2S is not so far from its precursors 0S, 1P1S and its postcursor 2P2S, so this leads to R_{SS} waveform's complication. On the other side, on Green's function $G_{r1}(t)$ for T component (T_{SS}) of SS waveform, the amplitudes of precursor 0S and postcursor 4S are much smaller than that of 2S. That's why the waveform of T_{SS} is mainly controlled by 2S and it's simple. So in this paper we only discuss the SS wave-train's complication is on the R_{SS}.

2.2 Relationship between crustal Green's function and thickness on bounce point and the distance

Figures 2a and 2b shows Green's function $G_{r1\_R}(t)$ and theoretical waveform R_{SS} under the condition of Δ=110° and H_{r1} increases from 10 km to 80 km, where zero point of time represents 2S, that is the original SS. The thicker H_{r1} is, the further the precursors and postcursors are from 2S (showed in Figure 2c), without strong change in amplitude.

Figures 2d, 2e and 2f shows the change of the shape of $G_{r1\_R}(t)$ and amplitude ratio of seismic phases when H_{r1}=40 km, and Δ increases from 40° to 180°. In this range of distance, the energy of 2S is increasing with Δ. The precursor 0S is weak and 1P1S is strong all the time. Although the postcursor 2P2S has a strong energy, it's amplitude decreases with Δ. Compared with 2S, the changing rules of arrival time difference with Δ for 0S, 1P1S and 2P2S are different from each other, but the change is not strong.

2.3 Relationship between SS wave-train's complication and crustal thickness on bounce point and the distance

We construct a source time function as below:

$$W(t) = (2/\tau)\sin^2(\pi t/\tau) \qquad 0 < t < \tau \tag{3}$$

This can be treated as the $S(t)$, which is the incident wave from the Moho beneath bounce point. If the source time τ lasts for 5 s, we can calculate SS wave-train under bounce point of Moho interface by $U^*_{SS}(t) = W(t) * G_{rl}(t)$, which is showed in Figures 2b and 2e. Notice that $U^*_{SS}(t)$ and $U_{SS}(t)$ are different. $U^*_{SS}(t)$ is just coming out of crust on bounce point. It is the shear

wave-train under Moho interface beneath SS reflection point and it does not reach the station. Here $G_{r1}(t)$ is Green's function for Figures 2a and 2d. From the result, we can see that even though the value of τ is so small, when H_{r1} is small (10~50 km), the original SS wave becomes complicated and the start time and polarity of this waveform are hard to be distinguished because of 1P1S. However, the peak energy of SS wave-train would move backward because of 2P2S. At the same time, the complication of wave-train is changing with different distances. In the real seismic record, the waves' energy is decreased and the higher frequency waves are attenuated during the propagation in the Earth. All of those elements lead to partial stacking of the phases 0S, 1P1S, 2P2S and 2S, which makes it difficulty to distinguish them from each other.

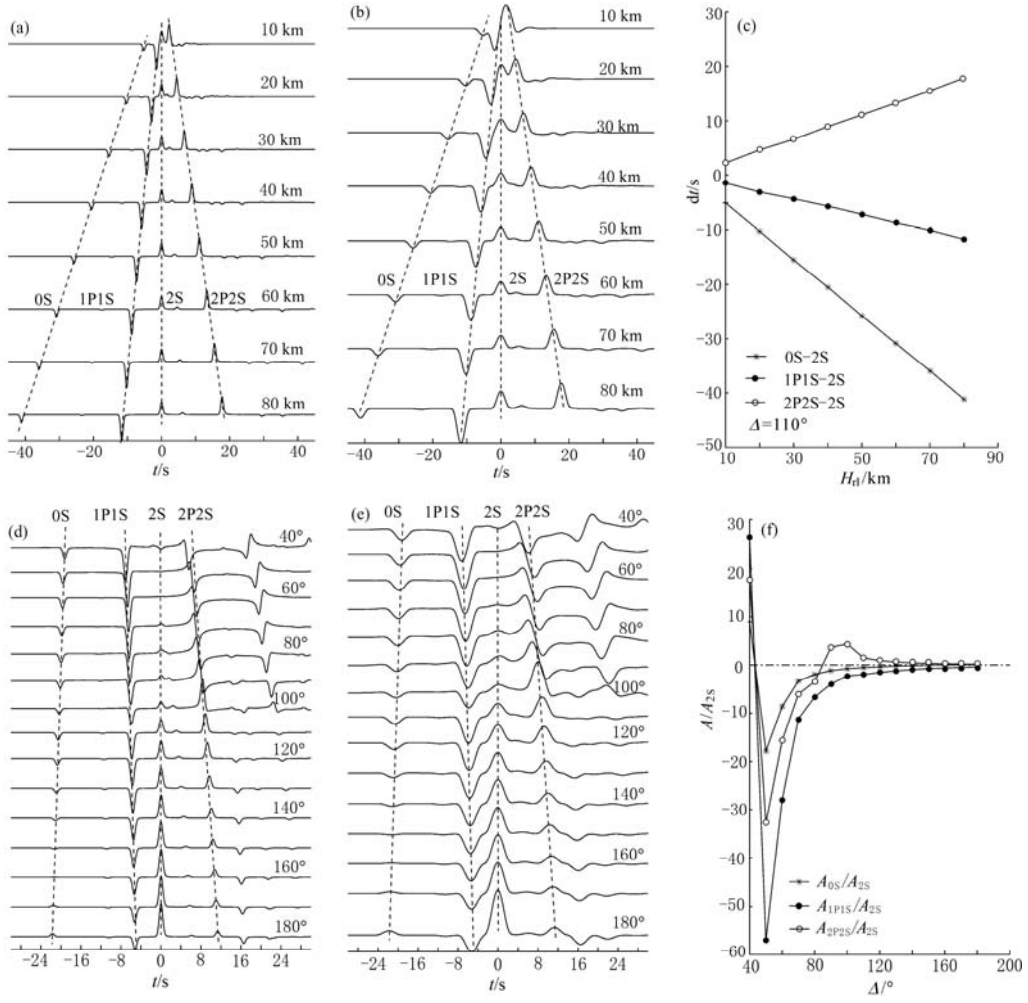

Figure 2 Green's functions and theoretical waveforms on *R* component at bounce point for different crustal thickness H_{r1} and distance Δ

(a) Green's function $R(t)$; (b) Theoretical waveform $U_{SS}^{*}(t)$; (c) Arrival time difference, respectively when Δ=110°, H_{r1} increases from 10 km to 80 km; (d) Green's funciton $R(t)$; (e) Theoretical waveform $U_{SS}^{*}(t)$; (f) Amplitude ratio of seismic phases, respectively when H_{r1}=40 km, and Δ increases from 40° to 180°. $U_{SS}^{*}(t)$ is the waveform recorded under Moho interface at bounce point. Zero time point is the response of 2S (SS). Other parameters of the model are the same as that in Figure 1

As shown in Figure 1a, although the time difference and amplitude ratio between 0S, 4S and 2S on T_{SS} are changing with H_{r1} and Δ, the energy they take are too weak to affect 2S, so the transverse wave-train is not that complicated.

2.4 Influence of velocity contrast at each side of Moho interface on SS waveform and splitting time beneath bounce point.

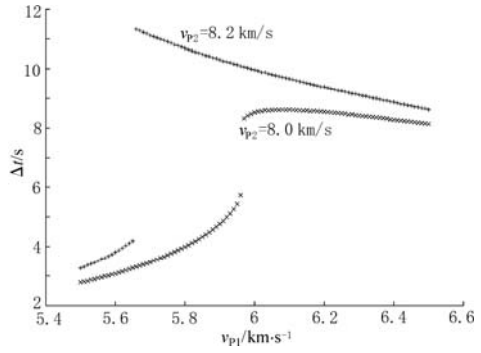

Figure 3 Relationship between wave velocity and splitting time for each side of Moho interface at the same crustal thickness
The crustal thickness H_{r1}=50 km and distance Δ=110°. Horizontal axis represents for the crustal average P velocity. Vertical axis represents for the splitting time between transverse component and radial component filtered by a bandwidth of 20 to 100 s according to Green's function calculated by theoretical model. P wave velocity increases from 5.5 km/s to 6.5 km/s; v_P/v_S is 1.732 in crust; P wave velocity is 8.2 km/s and 8.0 km/s beneath Moho interface

On the condition that the crustal thickness H_{r1}=50 km and the distance Δ=110°; the crustal average P wave velocity increases from 5.5 km/s to 6.5 km/s; v_P/v_S is 1.732; P wave velocity is 8.2 km/s and 8.0 km/s beneath Moho interface. Through calculating each model's Green's functions, waveforms are got by filtering the Green's function with a bandwidth of 20 to 100 s. At last, the splitting times between radial and transverse are measured by waveform's cross-correlation technique. It is showed in Figure 3 that with same crustal thickness, changing the average crustal velocity and velocity beneath Moho interface would cause great change in splitting time between $U^*_{SS}(t)$ transverse and radial for the different velocity contrast on each side of Moho interface. It also indicates that the splitting time between $U^*_{SS}(t)$ radial and transverse is mainly caused by crust thickness and velocity contrast on each side of Moho interface. When the average P wave velocity of inner crust v_{P1}>6 km/s, splitting time is not so sensitive to velocity change, in this case the splitting time includes more information about crustal thickness. When v_{P1}<6 km/s, no matter P wave velocity beneath Moho interface v_{P2} is 8.0 km/s or 8.2 km/s, the splitting time is sensitive not only to the crustal thickness but also to the change of velocity contrast.

3 Station crust and the complication of SS wave-train

3.1 Green's function for station crust

From the calculation above, the precursors and postcursors of SS generated by crustal response on bounce point have already caused the complication of SS wave-train. However, the waveform is recorded at seismic station; another important problem is what kind of effect crust beneath station would have on this complicated SS wave-train. The same model as Figure 1 is used to calculate Green's function beneath station, which can be seen in Figures 4a and 4b. It also shows the ray path of SS wave-train is transmitted to crust and recorded at seismic station in Figure 4c.

3.2 Influence of crustal thickness on SS wave-train's complication beneath station

The software Qseis5.6 is used to calculate synthetic seismogram. On the condition of the crustal thickness beneath bounce point are 10 km and 35 km, the crustal thickness on station H_{rc}

increase from 10 km to 80 km. The inner parameters of bounce point crust C_{r1} and station crust C_{rc} are same as what we use in 2.1, while the parameters beneath Moho interface is from IASP91 model (Kennett and Engdahl, 1991). The source moment tensor coefficients (Mrr: 5.20E+24, Mtt: –6.90E+24, Mpp: 1.70E+24, Mrt: –1.46E+25, Mrp: –2.96E–25, Mtp: –8.90E+24) of a real earthquake (time: 2005-03-19, 17h34min45.9s, location: 21.89°S, 179.56°W), which are gotten from Harvard CMT Catalog, are used in the calculation of theoretical seismogram. Source time function remains the function (3).

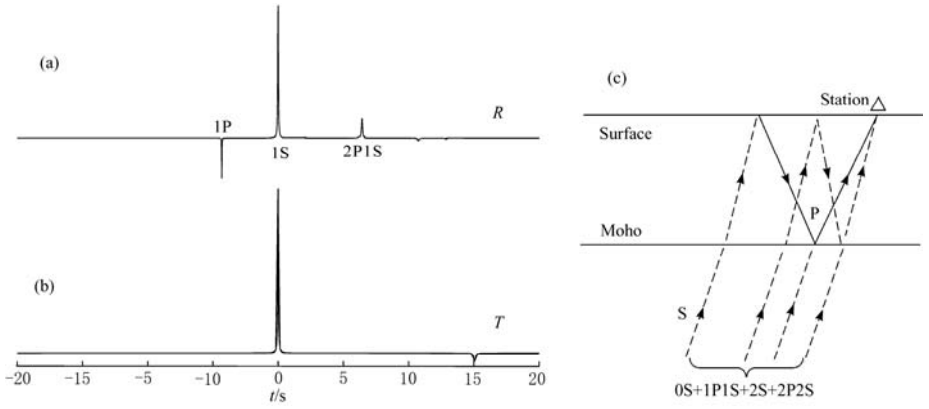

Figure 4 Green's function and schematic ray path for station crust
(a) and (b) are Green's functions of radial component and transverse component respectively. Several main phases are marked. 1P stands for incident S wave converts to P wave at Moho interface under station. 1S stands for S wave remains its phase after transmission at Moho interface. 2P1S stands for S wave becomes P wave twice and S wave once after it passes through Moho interface; (c) shows the ray path of SS wave-train in crust. Dash lines represent S wave, while solid lines represent P wave. Crustal thickness H_{rc} is 30 km. Distance Δ is 110°

As showed by Figure 5a, when Δ=110°, H_{rl}=10 km and H_{rc} increase from 10 km to 80 km, seismic phase 2P1S (traveling in the crust beneath station as P wave twice and S wave once) can be seen clearly on R_{SS} (see Figure 4). It is a set of seismic phases caused by the traveling of reverberation phase 2P2S of bounce point in the crust beneath the station. Because H_{r1} is very small and only 10 km, the phases of 0S, 1P1S, 2P2S related to the crust beneath the bounce point and 2S are combined together. The existence of 2P1S makes the whole wave-train longer and the whole waveform of wave-train changes with H_{rc}. When H_{r1} is larger, for example 35 km (see Figure 5b), 2P2S of the bounce point is strong and the following 2P1S is also strong. When $H_{rc}<H_{r1}$, 2P1S and 2P2S is so close and as a result, the waveform is changed and the period is enlarged. When $H_{rc}>H_{r1}$, the time difference between 2P1S and 2P2S is more and more large. While on the extreme condition of H_{rc}=80 km, the time difference reach about 17 s, which makes the whole wave-train longer. However, 2P1S's energy decreases rapidly as the distance increase, its effect on SS wave-train can be ignored when Δ reach 150° (see Figures 5c and 5d)

4 Disturbance to SS waveform by some adjacent seismic phases

Besides the contributions from the crust beneath the bounce point and the station to SS waveform's complication, there are some seismic phases with the same arrival time in different distances, which also disturb SS wave on the front and back side. To clarify the function of these phases, we assume the crustal thickness of bounce point and station is 40 km and parameters of

azimuth and hypocenter is the same as above. Then synthetic seismograms with distance from 40° to 180° are calculated using Qseis5.6.

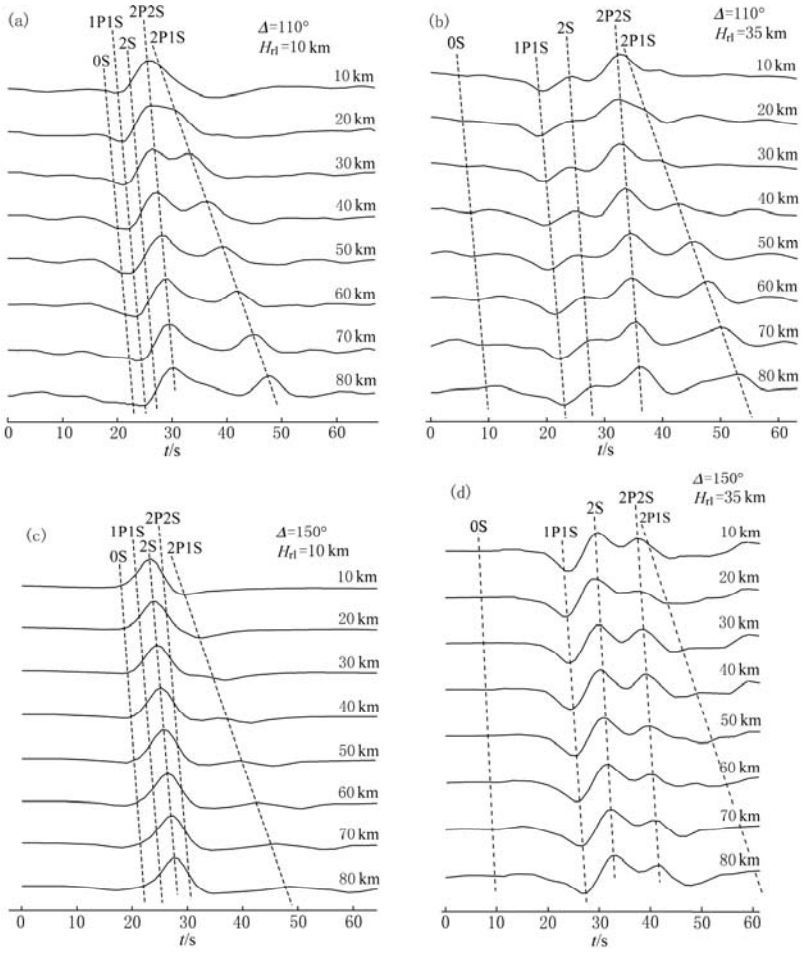

Figure 5 Station crustal thickness and complication of SS radial theoretical waveform

This figure shows the complication of SS radial waveform changes with crustal thickness increasing from 10 km to 80 km beneath station and Δ=110°, H_{r1}=10 km (a); Δ=110°, H_{r1}=35 km (b); Δ=150°, H_{r1}=10 km (c); Δ=150°, H_{r1}=35 km (d). Dash line corresponds with the theoretical arrival time for each phase's peak value. The seismic source parameters and medium model are illustrated in the paper

1) In the distance ranging from 40° to 50°, ScS phase disturbs the SS waveform in front of SS.

2) In the distance ranging from 40° to 75°, there are some waves from front and backside disturbing the waveform. On the distance around 80°, seismic phase *D* and SS waveforms arrive together to generate the complicated SS waveform.

3) In the distance ranging from 115° to 150°, there is an obvious seismic phase appearing on the backside of SS. After analyses with travel time and slowness, it can be recognized as SSP and SPS. The travel time is the same as that observed by Astiz *et al* (1996), which is got by stacking global seismic waveforms. In the one-dimension earth model, SSP and SPS have the same travel time, and they are close to SS together, so they could be the disturbances to R_{SS}.

4) In the distance ranging from 160° to 180°, a clear seismic phase *C* approaches SS from the backside and becomes a disturbance of the whole waveform.

Because the ray paths and polarization properties of seismic phases *A*, *B*, *C* and *D* are not analyzed accurately, they are just marked as these symbols.

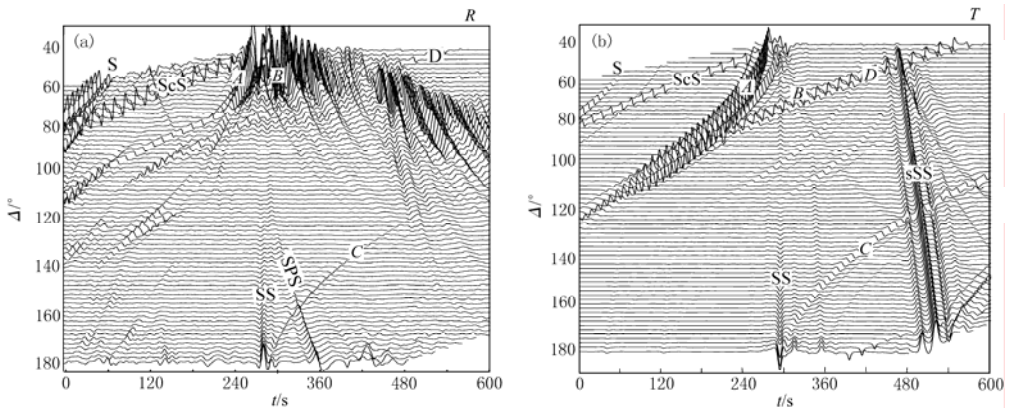

Figure 6 Synthetic seismogram of SS and adjacent seismic phases

(a) Synthetic seismogram on *R* component with distance from 40° to 180°; (b) Synthetic seismogram on *T* component with distance from 40° to 180°. The seismic source parameters and medium model are illustrated in the paper. According to SS theoretical arrival time based on IASP91 model, the waveforms are aligned. The seismic phases S, SS, ScS and sSS are marked. There are four unknown seismic phases marked as *A*, *B*, *C* and *D*

5 Possibility of estimating crustal thickness of bounce point by using splitting time of observed SS waveform

We chose two points with SS waveform's high signal-to-noise ratio, which are located in eastern and western China. The one in the east has a location at (118°E, 38°N) and there are 19 SS waveforms. Another one in the west has a location at (91°E, 36°N) and there are 46 SS waveforms. These waveforms are filtered by bandpass with a bandwidth from 20 to 100 s. Figures 7a and 7c are two cases for real waveform. We calculate the theoretical arrival time using IASP91 model, which can be seen as the dash line in Figures 7a and 7c. We choose time window for cross-correlation according to real waveforms, whose start-time t_1 and end-time t_2 can be seen in Figures 7a and 7c. We measure the splitting time of transverse and radial component using waveforms' cross-correlation, the result of which is shown in Figures 7b and 7d. After calculating the average of measured results, the splitting time of the eastern point and western point are about 4.4 s and 15.5 s separately. This indicates that the splitting time of western point with thick crust is obviously greater than that of the eastern point with thin crust. Our future work is to develop a new method: Using splitting time from observed waveform to calculate crustal thickness beneath bounce point accurately.

6 Discussion and conclusions

SS waveform's complication has been understood quantitatively by calculating synthetic seismograms for one deep earthquake and analyzing two sets of real waveform data. There are some conclusions made from this study.

1) S wave generates 1P1S and 2P2S of transmission-conversion and reflection-conversion on Moho interface and surface at the bounce point. They take a lot of energy, which cause SS waveform in *R*-component is more complicated than that in *T*-component. The complication has relationship with crustal thickness at bounce point, medium parameters and epicentral distance.

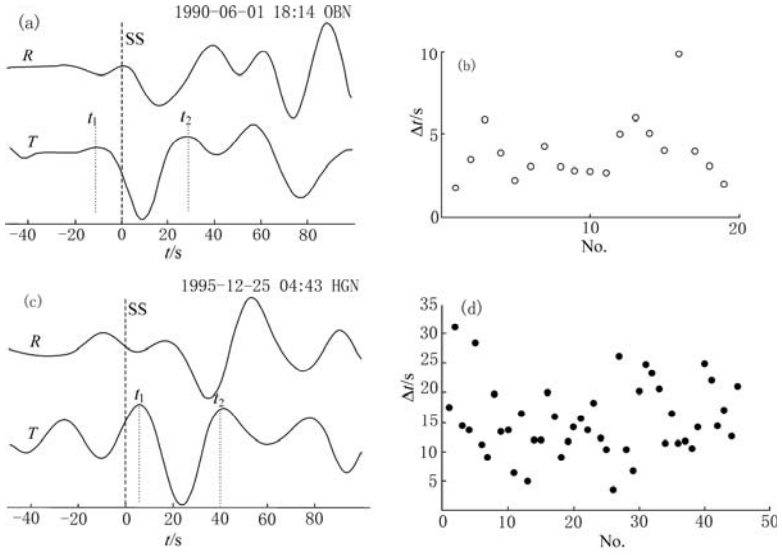

Figure 7 SS real recorded waveforms and splitting time measured from two sets of data
(a) and (c) are two real waveform cases respectively. The waveforms on above and below represent for radial and transverse component separately. The original source time and receiver station's name are marked. Dash line stands for the theoretical arrival time for SS from IASP91 model. t_1 and t_2 determine time windows for cross-correlation analysis. (b) and (d) are the measured results for data of bounce points at (118°E, 38°N) and (91°E, 36°N). Abscissa is serial No. of data. Ordinate is splitting time Δt

2) In the distance ranging from 40° to 150°, when the crust beneath bounce point is thinner, for example, the bounce point is in the ocean area, the response from both the crust beneath bounce point and seismic station should be considered. The response from crust beneath bounce point includes SS, the precursors 0S, 1P1S and postcursors 2P2S and 4S. The response from station crust is caused by 2P1S which is generated by 2P2S in the station crust. When the crust beneath bounce point is thicker, for example, the bounce point is in the continent area, 2P1S is far from wave-train generated by crust beneath the bounce point. Through choosing proper time window for SS wave-train, we can just consider the effect of the crust beneath bounce point on the response of SS waveform. In the distance ranging from 150° to 180°, the effect of seismic station crust can be ignored because 2P1S's energy is very weak.

3) In the distance ranging from 40° to 50°, ScS disturbs the waveform before SS wave arrives. In the distance ranging from 40° to 75°, seismic phases *A* and *B* disturb the waveform from backward. At distance around 80°, seismic phase *D* is intertwined with SS wave and become the complicated SS wave. In the distance ranging from 115° to 150°, the following seismic phase SSP and SPS disturb R_{SS}. In the distance ranging from 160° to 180°, seismic phase *C* approaches SS from the backward to become the disturbed waveform. So while using SS waveform data, these seismic phases disturbance should be avoided as much as possible. The data of SS waveform from distance 90° to 115° is suitable for studying. This conclusion has an instructional meaning in choo-

sing SS waveform data to measure crustal thickness and seismic anisotropy splitting parameters at bounce point, and so on.

4) When P-wave velocity in the crust is greater than 6 km/s, the observed splitting time Δt is dependent on the crustal thickness H_{r1} beneath the bounce point. Through the analysis of real SS waveforms, the observed Δt has an obvious positive correlation with H_{r1} beneath the bounce point. It means the splitting time at the bounce point with thick crust is greater than that with thin crust. So H_{r1} can be evaluated by finding the quantitative relationship between Δt and H_{r1}.

From the above analyses, R_{SS} waveform is very complicated and it includes plenty of information, such as crustal thickness at bounce point and at seismic station, average wave velocity in crust, and so on. After considering the crustal responses from bounce point and seismic station separately, SS waveform can be understood thoroughly. Only the correct theoretical knowledge can help to extract crustal information in certain area from a sea of waveform data. It is hopeful that a new method for measuring crustal thickness could be developed by using SS waveform's splitting time.

In this paper, deep earthquake is chosen to simplify the influence of medium around hypocenter on SS waveform. If SS waveform with shallow hypocenter is used, the influence on waveform from hypocenter area should also be considered and calculated. This paper doesn't discuss the complication of SS waveform with distance less than 40°. It's because the existence of the slow-velocity zone in upper mantle causing the triplication of S wave. On the other hand, different SS waveforms appear in the same distance with one seismic source, but at different azimuth. This complication caused by the diversity of source radiation patterns is also not mentioned in this paper. In addition, the observed data have noises, so other techniques should be adopted, such as filtering, stacking, and so on, in order to reduce the noise except choosing data with high signal noise ratio, which will be discussed in another paper.

Acknowledgements We should give more acknowledgements to Drs. WANG Rong-jiang and YUAN Xiao-hui for their help. ZHOU Zhe and ZHU Gui-zhi made an English proof for the paper. To analyze waveform, Matseis developed by Sandia National Laboratory and SAC2000 developed by Lawrence Livermore National Laboratory are used. Editors and anonymous reviewers made valuable comments on the manuscript. All of these contributions are gratefully acknowledged.

References

Astiz L, Earle P S, Shearer P M. 1996. Global stacking of broadband seismograms [J]. *Seism Res Lett*, **67**(4): 8-18.

Bhattacharyya J, Masters G, Shearer P. 1996. Global lateral variations of shear wave attenuation in the upper mantle [J]. *J Geophys Res*, **101**(B10): 22 273-22 289.

Grand S P. 2002. Mantle shear-wave tomography and the fate of subducted slabs [J]. *Phil Trans R Soc Lond A*, **360**: 2 475-2 491.

Kennett B L N and Engdahl E R. 1991. Traveltimes for global earthquake location and phase identification [J]. *Geophys J Int*, **105**: 429-465.

Lawrence J F and Shearer P M. 2006. A global study of transition zone thickness using receiver functions [J/OL]. *J Geophys Res*, **111**: B06307. doi: 10.1029/2005JB003973.

Ma Y, Wang R, Zhou H. An improvement to the orthonormalization method for efficient computation of plane-wave response in multi-layered medium [J]. *Journal of the Graduate School of the Chinese Academy of Sciences*, **25**(1): 47-53.

Reid F J L, Woodhouse J H, Heijst H J. 2001. Upper mantle attenuation and velocity structure from measurements of differential S phases [J]. *Geophys J Int*, **145**: 615-630.

Schmerr N and Garnero E. 2006. Investigation of upper mantle discontinuity structure beneath the central Pacific using SS precursors [J/OL]. *J Geophys Res*, **11**: B08305. doi: 10.1029/ 2005JB004197.

Wang R. 1999. A simple orthonormalization method for stable and efficient computation of Green's functions [J]. *Bull Seism Soc Amer*, **89**: 733-741.

Wolfe C J and Silver P G. 1998. Seismic anisotropy of oceanic upper mantle: Shear wave splitting methodologies and observations [J]. *J Geophys Res*, **103**(B1): 749-771.

Yang X and Fischer K M. 1994. Constraints on North Atlantic upper mantle anisotropy from S and SS phases [J]. *Geophys Res Lett*, **21**(4): 309-312.